Endosomal localization and function of sorting nexin 1

Qi Zhong*†, Cheri S. Lazar*†, Hélène Tronchère*, Trey Sato‡, Timo Meerloo‡, Michele Yeo*, Zhou Songyang§, Scott D. Emr‡, and Gordon N. Gill*‡¶

Departments of *Medicine and ‡Cellular and Molecular Medicine, University of California at San Diego School of Medicine, La Jolla, CA 92093-0650; and §Department of Biochemistry and Molecular Biology, Baylor College of Medicine, Houston, TX 77030

Communicated by Marilyn Gist Farquhar, University of California at San Diego, La Jolla, CA, March 12, 2002 (received for review November 20, 2001)

There are 17 human members of the sorting nexin (SNX) family of proteins that contain Phox (PX) domains. Yeast orthologs function in vesicular trafficking and mammalian proteins have been implicated in endocytic trafficking of cell surface receptors. The first member of this family, SNX1, was identified via interaction with the epidermal growth factor receptor. The present studies indicate that SNX1 and SNX2 are colocalized to tubulovesicular endosomal membranes and this localization depends on PI 3-kinase activity. Point mutations in the PX domain that abolish recognition of phosphorylated phosphatidylinositol (PtdIns) *in vitro* abolish vesicle localization *in vivo* indicating that lipid binding by the PX domain is necessary for localization to vesicle membranes. Deletion of a predicted coiled-coil region in the COOH terminus of SNX1 also abolished vesicle localization, indicating that this helical domain, too, is necessary for SNX1 localization. Thus, both PX domain recognition of PtdIns and COOH terminal helical domains are necessary for localization of SNX1 with neither alone being sufficient. Regulated overexpression of the NH_2 terminus of SNX1 containing the PX domain decreased the rate of ligand-induced epidermal growth factor receptor degradation, an effect consistent with inhibition of endogenous SNX1 function in the endosome compartment. SNX1 thus functions in regulating trafficking in the endosome compartment via PX domain recognition of phosphorylated PtdIns and via interaction with other protein components.

Regulated targeting of proteins to appropriate sites of action within cells is accomplished in part by enzymatic modification of the address site that is recognized by modular protein domains. Phox (PX) domains are ≈120-residue protein modules initially recognized by sequence homology in NADPH oxidase subunits, sorting nexins, and PI 3-kinases (1). Proteins containing PX domains are associated with specific membrane compartments, and the PX domains of Vam7p, $p40^{Phox}$, $p47^{Phox}$, CISK, and sorting nexin (SNX) 3 recognize specific phosphatidylinositol (PtdIns) (2–8). All PX domains of yeast are reported to recognize PtdIns (3) P (9). Binding affinities of the yeast proteins, however, differ up to 10^3-fold *in vitro*, suggesting that membrane association *in vivo* depends on additional protein·protein interactions (9).

SNX1, initially identified via its interaction with epidermal growth factor receptor (EGFR), contains a PX domain in its NH_2 terminus and three predicted coiled-coils in its COOH terminus (10). Other SNX family members also contain coiled-coils (SNX2 and SNX4), contain little sequence beyond a PX domain (SNX3), or contain various functional domains (an RGS domain in SNX13/RGS-PX1, an SH3 domain in SNX9) (11–14). hSNX1 interacts with orthologs of three yeast proteins that together with Vp5p, the yeast ortholog of SNX1, form the retromer complex, suggesting conservation of function in vesicular trafficking in the endocytic system (15, 16).

We have analyzed the role of the PX and coiled-coil domains of SNX1 in subcellular localization to tubulovesicular structures and in interactions with SNX family members. We assessed the effects of regulated overexpression of the NH_2 terminus of SNX1 that contains the PX domain on ligand-induced down-regulation of EGFR. The results of these studies indicate that both an intact PX domain that recognizes PtdIns lipids and the coiled-coil domains of SNX1 involved in protein·protein interactions are required for proper vesicle membrane targeting. Neither domain alone is sufficient. We conclude that SNX1 functions to enhance EGFR trafficking in the endosome to lysosome pathway.

Materials and Methods

Rabbits were immunized with the purified PX domain of SNX1 (aa 142–269) and the resultant antisera that was affinity purified (8501) specifically recognized SNX1 but not SNX2 or SNX3. The SEFIGA rabbit polyclonal antibody was generated using a peptide corresponding to the COOH terminus of hEGFR.

Protein Expression, Purification, and Characterization. Sequences encoding PX domains were amplified in PCR reactions from cDNAs encoding the indicated proteins, digested using appropriate restriction enzymes and cloned into expression vectors. Mutations were prepared using oligonucleotide-directed mutagenesis and verified by sequencing. Proteins were expressed in *Escherichia coli* and soluble proteins were purified on the appropriate affinity columns (NTA, Glutathione, or Chitin agarose) and chromatographed on a Superdex S200 column. Crosslinking of the SNX1 PX domain was carried out using increasing concentrations of glutaraldehyde at 25°C for 5 min and reactions were terminated by adding SDS/PAGE sample loading buffer.

Analytical ultracentrifugation analysis of the SNX1 PX domain (0.715 mg/ml, OD_{280} = 0.25) was carried out using a Beckman Optima XL-1 instrument and the data were analyzed using the XL-A/XL-1 data analysis software (Beckman Instruments).

Protein·Lipid Overlay Assays. Protein·lipid overlay assays were based on the procedure described by Dowler *et al.* (17). Membrane arrays spotted with 100 pmol of the indicated phospholipids were obtained from Echelon Research Laboratories (Salt Lake City). The PX domain of SNX1 was detected with the affinity-purified antibody (8501) used at 1:1,000 dilution. GST-PX fusions were detected with an anti-GST mouse monoclonal antibody at 1:500 dilution (Santa Cruz Biotechnology). After washing, anti-rabbit or anti-mouse antibody-horseradish peroxidase conjugates were added for 1 h at 1:3,000 dilution. Membranes were washed and developed for enhanced chemiluminescence.

Immunofluorescence and Immunoelectron Microscopy. Cells grown on coverslips were fixed in 2% paraformaldehyde, neutralized,

Abbeviations: SNX, sorting nexin; HA, hemagglutinin; PX, Phox; EGFR, epidermal growth factor receptor; PtdIns, phosphatidylinositol.

†Q.Z. and C.S.L. contributed equally to this work.

¶To whom reprint requests should be addressed. E-mail: ggill@ucsd.edu.

The publication costs of this article were defrayed in part by page charge payment. This article must therefore be hereby marked "*advertisement*" in accordance with 18 U.S.C. §1734 solely to indicate this fact.

CELL BIOLOGY

and blocked using 2.5% FCS/PBS. For the monoclonal primary antibodies (anti-LAMP, anti-EEA1, and anti-FLAG) a goat anti-mouse IgG H+L chains conjugated to Alexa Fluor 594 (Molecular Probes) was used. The polyclonal anti-hemagglutinin (HA) antibody was followed by goat anti-rabbit IgG H+L chains conjugated to Alexa Fluor 488. Omission of primary antibodies were used as negative controls. The coverslips were viewed using a ×63/1.4 N.A. Zeiss oil immersion objective on a Zeiss Axioskop fluorescence microscope equipped with a 640 × 480 pixel COHU Interline Transfer CCD Camera (Cohu, San Diego).

Deconvolution microscopy images were captured with a DeltaVision deconvolution microscope (Applied Precision, Issaquah, WA). In general, 20 optical sections spaced by 0.2 μm were taken using a ×100 (N.A. 1.4) lens. The data sets were deconvolved and analyzed using SOFTWORX software (Applied Precision) on a Silicon Graphics (Mountain View, CA) Octane work station.

For immunogold labeling, cells were fixed in freshly prepared formaldehyde in 100 mM sodium phosphate buffer (pH 7.4) and prepared for ultrathin cryosectioning as described (18). SNX1 was detected using rabbit polyclonal antibody 3904 (10), followed by a 10-nm gold conjugated goat anti-rabbit antibody. Transferrin receptors were detected using a mouse monoclonal antibody (clone H68.4 from Ian Trowbridge, Salk Institute, La Jolla, CA), followed by 5-nm gold conjugated goat anti-mouse. Sections were observed and photographed on a JEOL 1200 EXII transmission electron microscope.

Mammalian Cell Expression and Coimmunoprecipitation. Full-length or mutant SNX proteins were cloned into pcDNA3 expression vectors (Invitrogen) engineered to contain an in frame HA-or FLAG-epitope tag at the NH_2 terminus. Proteins were also subcloned into the pEGFPC1 expression vector (CLONTECH) to provide an in-frame GFP reporter. NH_2 and COOH terminal constructs of SNX1 and SNX2 were prepared using PCR. Mutations were prepared by standard techniques and all of the constructs were verified by sequencing. The HA-tagged NH_2-terminal fragment of SNX1 (SNX1–1N, aa 1–325) was cloned into the pUHG derivative of the tet-off system and transfected into HeLa cells containing the integrated tTA gene (19). Clonal lines were selected and maintained in 2 μg/ml tetracycline and induced by removal of tetracycline for 16–36 h.

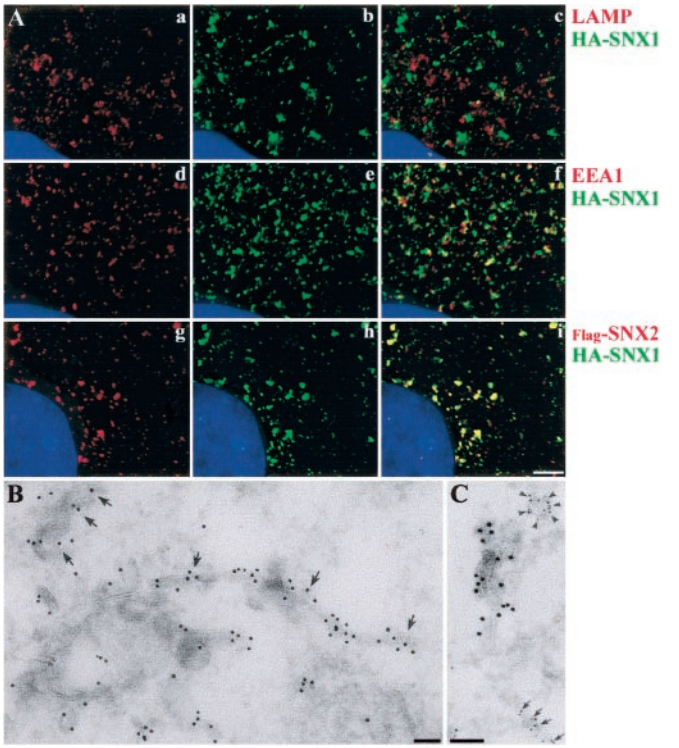

Fig. 1. Subcellular localization of SNX1. (*A*) Immunofluorescence microscopy of SNX1 and SNX2. HA- and FLAG-epitope-tagged SNX proteins were expressed in COS7 cells. Immunofluorescence deconvolution microscopy with volume reconstruction was performed using anti-HA and anti-FLAG antibodies and the nucleus was visualized with DAPI. *c*, *f*, and *i* are merged images. SNX1-containing vesicles are distinct from lysosomes (*c*); a fraction of SNX1 are coincident with EEA1-positive early endosomes, but many are distinct (*f*). There is extensive colocalization of SNX1 and SNX2 (*i*). (Scale bar, 1 μm.) (*B*) Immunoelectron microscopy of SNX1. SNX1 was identified in stable expresser CV1 cells by using an affinity-purified rabbit polyclonal antibody (Ab3904) that recognizes the COOH terminus of SNX1. Visualization was with 10-nm gold particles. (Scale bar, 0.1 μm.) (*C*) Comparison of the localization of SNX with TfR. Transferrin receptors were detected using a mouse monoclonal antitransferrin antibody and 5-nm gold particles; SNX1 was visualized using 10-nm gold particles. (Scale bar, 0.1 μm.)

Results

Determinants of the Subcellular Localization of SNX1. SNX1 is localized to intracellular vesicles that are distinct from the endoplasmic reticulum, lysosomes, and Golgi (Fig. 1 *Aa–Ac* and data not shown). As shown in Fig. 1 *Ad–Af*, SNX1 vesicles partially overlap but are not strictly identical with EEA1-positive early endosomes. Immunoelectron microscopy indicated that SNX1 is present both on vesicles and on tubulovesicular structures (Fig. 1*B*). These structures are largely distinct from those containing transferrin receptors (TfR) (Fig. 1*C*). Less than 20% of SNX1-containing vesicular structures had TfR and only 8% of TfR vesicles contained SNX1. Coexpressed SNX1 and SNX2 localized in the same vesicular structures by immunofluorescence (Fig. 1 *Ag–Ai*) and by immunoelectron microscopy (data not shown). SNX1 and SNX2 are thus localized to the membranes of tubulovesicular structures that are part of the early endocytic compartment, but which are partially distinct from previously defined EEA1- and recycling TfR-containing endosomes.

The specific binding of the PX domains to PtdIns predicted that the subcellular localization of SNX1 may depend on PI 3-kinase activity. To assess this, the PI 3-kinase inhibitor LY294002 was added to COS7 cells expressing GFP-SNX1, and its subcellular distribution was compared with that seen in untreated cells. Inhibition of PI 3-kinase activity resulted in loss of vesicle association (Fig. 2, uppermost right panel), suggesting that the generation of 3-phosphoinositides is necessary for SNX1 endosomal localization. To determine whether the PX domain was necessary for localization to these vesicles, aa 181–266 were deleted from the 522-residue SNX1 protein (ΔPX SNX1). In contrast to WT SNX1, this mutant was diffusely expressed in the cytoplasm, indicating that an intact PX domain is necessary for proper vesicle targeting (Fig. 2, ΔPX). Structural features that are conserved among PX domains of SNX proteins include the two Arg-rich clusters, RRFSD and RRXXL, and a Pro-rich sequence, PXXP (see Fig. 4). Point mutations in these residues in holo SNX1 abolished vesicle localization of the protein (Fig. 2). Vesicular membrane localization of SNX1 thus depends on an intact PX domain and on the PI 3-kinase activity that generates the target PtdIns.

Deletion of a predicted coiled-coil region in the COOH terminus (ΔC, which deleted aa 355–387) similarly abolished vesicle localization of SNX1 (Fig. 2, ΔC2). Vesicular localization of SNX1 thus depends on an intact PX domain, on its lipid target, and on an intact COOH terminus. The observation that deletion of a coiled-coil region of the COOH terminus of holo SNX1 abolished vesicle localization suggested that the PX domain of SNX1, although

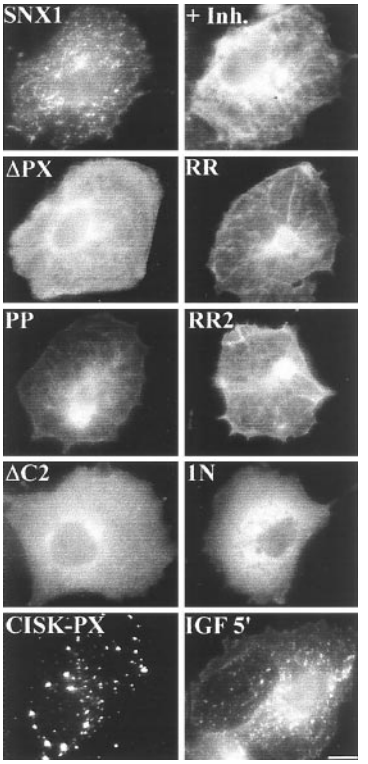

Fig. 2. Structural features that determine the subcellular localization of SNX1. GFP-SNX1 and GFP-mutant SNX1 were expressed in COS-7 cells and visualized by fluorescence microscopy. WT SNX1 + Inh = WT SNX1 in cell treated with 50 μM LY 294002 for 1 h; ΔPX SNX1, deletion of residues 181–266; RR = R185G, R186S SNX1; PP = P209A, P210A SNX1; RR2 = R238L, R239G SNX1; ΔC2 = deletion of aa 355–387 (coil 2); 1N = SNX1–1N (aa 1–325); CISK-PX domain (aa 1–121); +IGF 5′ = WT SNX1 in cells treated with IGF-1 for 5 min. Similar results were observed over a time course of 2–30 min and in cells treated with EGF and LPA (not shown). (Scale bar, 5 μm.)

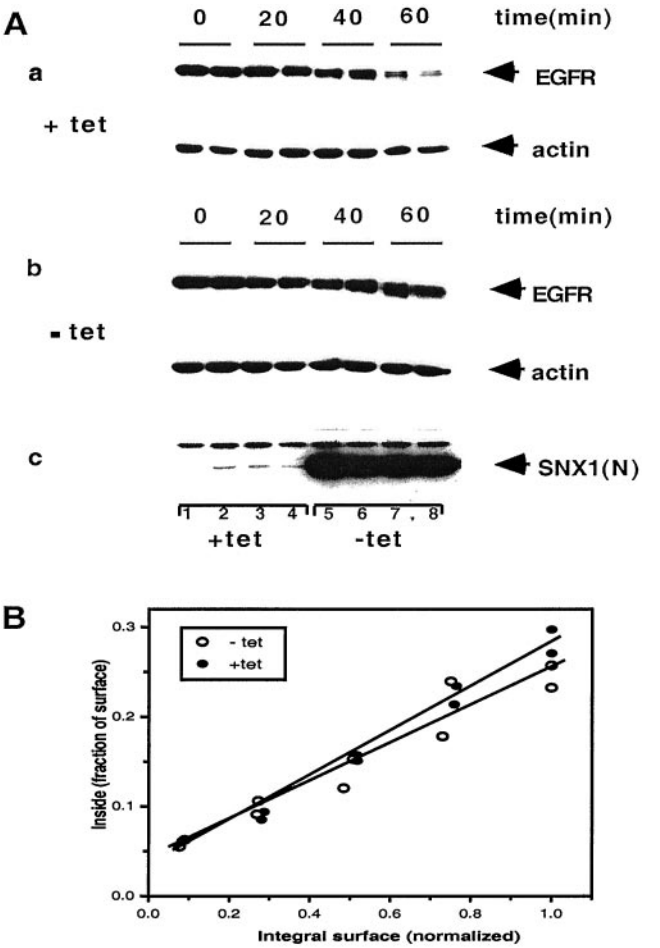

Fig. 3. Effects of overexpression of the PX domain of SNX1 on ligand-induced down-regulation of EGFR. (*A*) Effects on EGFR mass. HeLa cells expressing HA-SNX1–1N were maintained with or without tetracycline for 36 h. before addition of 100 nM EGF. At the indicated times cells were lysed and EGFR mass was analyzed by Western blotting using the SEFIGA antibody. Actin served as an internal loading control. (*a*) With tetracycline; (*b*) without tetracycline; (*c*) detection of HA-SNX1–1N with anti-HA antibody. (*c*) Lanes 1 and 5, before adding EGF; lanes 2 and 6, 20 min after EGF; lanes 3 and 7, 40 min after EGF; lanes 4 and 8, 60 min after EGF. Similar results were obtained in three additional experiments in which the mass of EGFR in the presence of HA-SNX1–1N was 2–3-fold greater than that without HA-SNX1–1N (range of receptor mass remaining at 30–60 min after adding EGFR averaged 50–68% in the presence of HA-SNX1–1N vs. 20–24% in its absence). (*B*) Effects of the PX domain of SNX1 on the rate of internalization of EGF. Endocytic rate constants were determine as described by Wiley and Cunningham (22). EGF was added at 2 ng/ml. ●, with tet; ○, without tet.

necessary, was not sufficient for subcellular localization. This was confirmed by finding diffuse localization of the PX domain of SNX1 (SNX1–1N) (Fig. 2, 1N). In contrast, the PX domains of other proteins are sufficient for vesicle localization. SNX3, which consists principally of a PX domain, is localized to early endosomes (6), as is the PX domain of CISK (Fig. 2, lowest left panel). Treatment of cells with agents that activate PI 3-kinase (IGF-1, EGF, LPA) did not alter the subcellular localization of SNX1 (Fig. 2, lowest right panel). These agents also failed to alter the diffuse localization of SNX1–1N (data not shown).

Effect of Overexpression of the PX Domain of SNX1 on Down-Regulation of EGFR. A role for SNX1 in endosome trafficking was implied from studies indicating that overexpression of SNX1, which recognized the lysosomal targeting sequence code in EGFR, decreased cellular EGFR levels (10). To assess the effects of SNX1 on trafficking of EGFR in the endosomal compartment, we expressed the HA-tagged NH_2 terminus of SNX1 containing the PX domain (SNX1–1N, aa 1–325) in HeLa cells under control of the tetracycline repressor/activator (19) and compared the rate of EGF-induced receptor degradation in the presence and absence of this putative inhibitor of SNX1. As shown in Fig. 3*A*, expression of SNX1–1N resulted in a decreased rate of ligand-induced EGFR degradation. The rate of self-phosphorylated receptor loss was also decreased (data not shown), consistent with a delay in inactivation and movement through the endosome compartment to lysosomes (20). The mechanism underlying this effect is uncertain. Ligand binding and activation of EGFR increases the rate of endocytosis ≈10-fold (21). Comparison of the rates of internalization of ^{125}I-EGF without and with overexpression of SNX1–1N revealed no significant difference in the endocytic rate constants (Fig. 3*B*). The average k_e values of 0.25 and 0.21 are equivalent to those reported elsewhere (21, 22).

Overexpression of SNX1–1N could compete with targeting of endogenous SNX1 to membranes or could induce formation of aberrant protein complexes (see Fig. 4). Additionally, overexpression of some SNX proteins—i.e., SNX3 and SNX15—results in aberrant endosomal vesicle formation (6, 23). However, early endosome morphology, as assessed by immunofluorescence and immunoelectron microscopy, was not changed by overexpression of SNX1–1N (data not shown). It is thus likely that the NH_2 terminus containing the PX domain of SNX1 interferes with

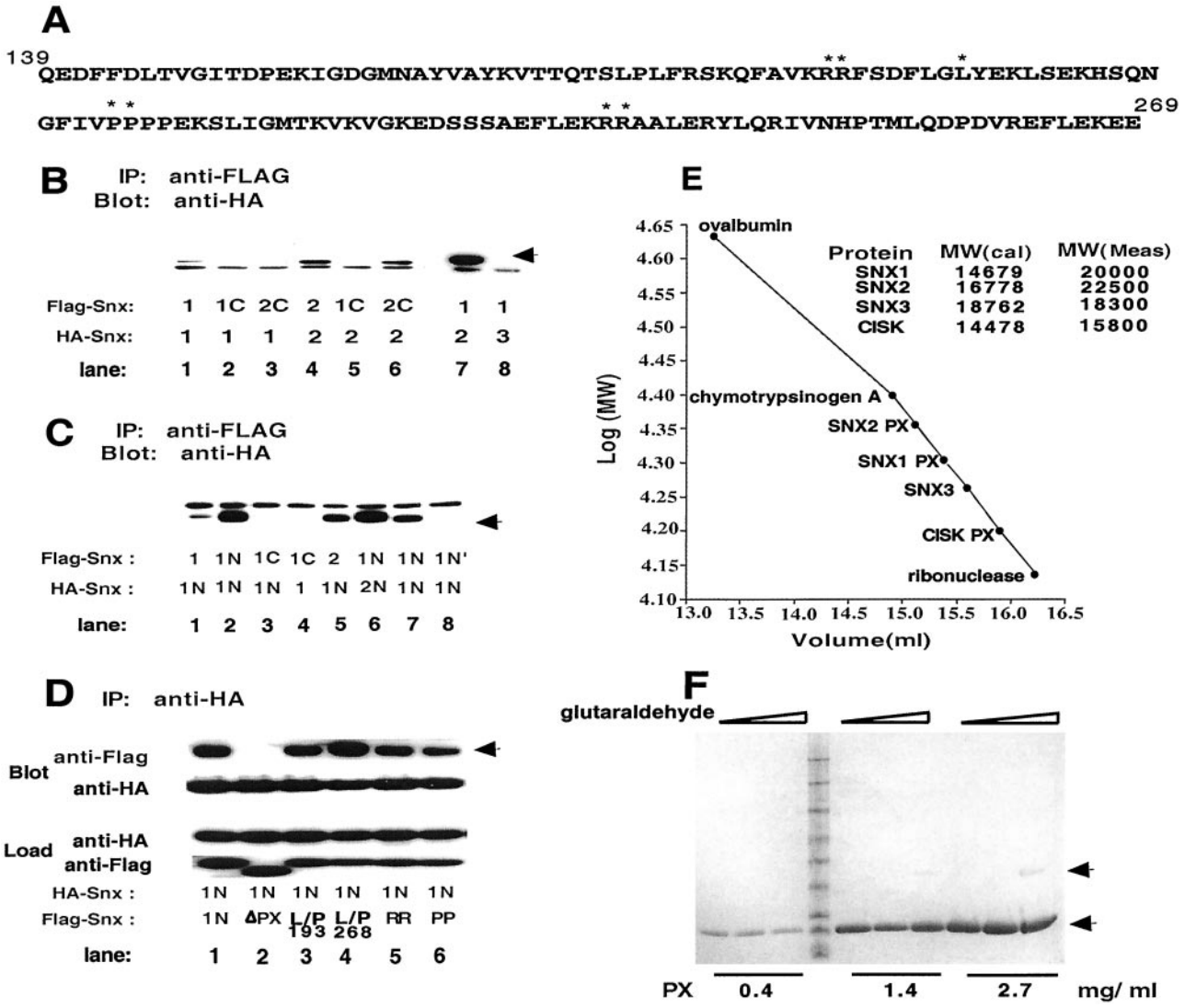

Fig. 4. The PX domain of SNX1 forms dimers. (*A*) Sequence of the PX domain of SNX1. Residues that were mutated are indicated by *. (*B–D*) Analysis of SNX complex formation. Various SNX proteins or fragments of these containing HA or FLAG epitope tags were coexpressed in HEK 293 cells. FLAG-tagged proteins were immunoprecipitated, solubilized, and analyzed by Western blotting with anti-HA antibody to detect complexes. 1, SNX1; 2, SNX2; 3, SNX3; 1N, aa 1–325 of SNX1; 2N, aa 1–325 of SNX2; 1C, residues 296–522 of SNX1; 2C, aa 296–519 of SNX2; N′, aa 1–140 of SNX1; ΔPX, SNX1–1NΔ aa 181–266; RR, 185G, R186S; PP, P209A, P210A. Expression of HA- and FLAG-tagged proteins were verified for all experiments and the amount of direct immunoprecipitated protein was determined for each experiment. Representative controls are shown in *D*. The load represents 5% of the sample. Assuming equivalence of antibody detection, 25–50% of partner proteins were coimmunoprecipitated with the directly immunoprecipitated protein as determined by densitometry. (*E*) Gel filtration chromatography of the PX domain of SNX1. The PX domains of SNX1 (residues 142–269), SNX2 (aa 118–266), and CISK (aa 1–121) and SNX3 (aa 1–162) were expressed in *E. coli* by using the self-cleaving intein system. Protein was analyzed by FPLC on Superdex G-75. (*F*) Glutaraldehyde crosslinking of the PX domain of SNX1. Increasing concentrations of glutaraldehyde (0.5–1,200 μM) were added to the indicated concentrations of purified PX domain. After incubation protein was analyzed on SDS/PAGE.

localization of endogenous SNX1 and SNX1-dependent trafficking of EGFR without distorting the endosome compartment (24).

SNX Protein Complexes. Colocalization of SNX1 and SNX2 *in vivo* is consistent with reported interactions among SNX family proteins (11, 24). Determinants of the *in vivo* interaction between SNX1 and SNX2 were assessed by coimmunoprecipitation of epitope-tagged SNX1, SNX2, and fragments of these in HEK 293 cells. As shown in Fig. 4 *B* and *C*, SNX1 and SNX2 form homo- and heterodimers (see also ref. 11). SNX2 appears to homodimerize more strongly than SNX1 (Fig. 4*B*, lane 4 vs. lane 1), due in part to forces contributed by the coiled-coil-containing COOH terminus of SNX2 (Fig. 4*B*, lane 6 vs. lane 2). SNX1 and SNX2 heterodimerize strongly, but neither interacts with SNX3 (Fig. 4*B*, lanes 7 and 8). The NH_2 terminus containing the PX domains of both SNX1 and SNX2 contributed to dimerization (Fig. 4*C*). The NH_2 terminus of SNX1 dimerizes with SNX1, with itself, with SNX2, and with the NH_2 terminus of SNX2 (Fig. 4*C*, lanes 1, 2, 5, 6, and 7). The NH_2 terminus proximal to the PX domain of SNX1 (residues 1–140) does not interact (Fig. 4*C*, lane 8), indicating that the PX domain contributes interacting forces to SNX1 and SNX2. Deletion of a large portion of the PX domain (ΔPX, aa 181–266) disrupted dimerization of the NH_2-terminal fragments of SNX1 (Fig. 4*D*). However, point mutations that abrogate vesicle localization *in vivo* (Fig. 2) and PtdIns binding *in vitro* (see Fig. 5) did not affect interactions involving the PX domain-containing NH_2 terminus of SNX1 (Fig. 4*D*).

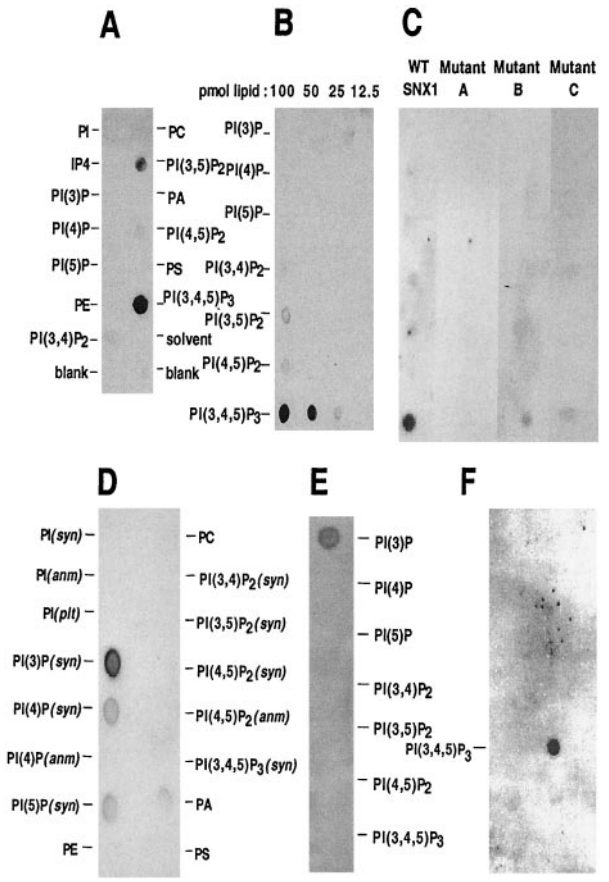

Fig. 5. Analysis of lipid binding of the PX domain of SNX proteins. (*A* and *B*) Specificity of lipid binding of SNX1. Nitrocellulose membrane arrays that contained the indicated concentrations of phospholipids were incubated with 0.1 μg/ml of the purified PX domain of SNX1 (aa 142–269) and bound protein was detected using the 8501 antibody. In *A* 100 pmol of each lipid were spotted. In *B* the indicated concentration of each PtdIns is given at the top of the panel. (*C*) Effects of mutations on lipid binding. Mutations in the PX domain of SNX1 are: A, R185G, R186S; B, P209A, P210A; C, R238L, R239G. WT and each of the purified mutant PX domains of SNX1, produced via intein cleavage (aa 142–269), were used at 0.2 μg/ml on strips containing 100 pmol of each PtdIns. The ability of the anti-PX antibody (8501) to detect the mutant proteins was verified by Western blotting. (*D*) Specificity of lipid binding of SNX1. GST-PX domain of SNX2 (aa 118–266) (0.3 μg/ml) was used in lipid overlay assays where each spot contained 100 pmol of lipid, and specific binding was detected using a monoclonal anti-GST antibody. (*E*) Binding specificity of the PX domain of SNX3. GST-SNX3 (0.4 μg/ml) was incubated with nitrocellulose strips containing 100 pmol of each of the indicated PtdIns. (*F*) Binding specificity of the PH domain of Grp1. GST-PH domain (2.0 μg/ml) was incubated with 100 pmol of lipids arrayed as in *D*.

Thus, the interaction interface is not congruent with the PtdIns binding surface, and dimerization *per se* is not sufficient for vesicle localization of SNX1.

The purified PX domain of SNX1 (aa 142–269) migrated as a larger species than its calculated molecular weight, as did the PX domain of SNX2 (aa 118–266) (Fig. 4*E*). In contrast, the migration of SNX3 and the PX domain of CISK corresponded to their calculated molecular weights. The migration of the PX domains of SNX1 and SNX2 on gel filtration is compatible with asymmetric molecules (prolate elipsoid rather than globular). To determine whether the PX domain directly dimerized, the PX domain of SNX1 was analyzed using analytical ultracentrifugation. A single species was detected with a molecular weight of 14,525 Da that corresponds to the calculated monomer molecular weight of 14,679. Crosslinking using a wide range of glutaraldehyde revealed only a trace of dimer formation (Fig. 4*F*). Because the purified PX domain does not directly dimerize, strong homo- and heterodimerization of SNX1 and SNX2 *in vivo* involves both the PX and COOH termini and most likely reflects formation of complexes that include other proteins analogous to formation of the retromer complex (15, 16).

PX Domain Recognition of PtdIns. Because vesicle membrane localization of SNX1 depends on PI 3-kinase activity, phosphorylation of the D3 position of the inositol ring was predicted to be a major determinant of PX domain recognition of membrane lipids. We thus tested the ability of the PX domain of SNX1 to bind various phospholipids, using a protein·lipid overlay assay (17). As shown in Fig. 5*A*, the PX domain of SNX1 specifically recognized PtdIns (3,5) P_2 and PtdIns (3,4,5) P_3. There was no detectable binding to monophosphorylated PtdIns nor to phosphatidylcholine (PC), phosphatidylinositol (PI), phosphatidylserine (PS), or phosphatidic acid (PA). PtdIns (3,4,5) P_3 was the major lipid bound with lesser binding to PtdIns (3,5) P_2 detected. Using higher amounts of PX domain protein, binding to PtdIns (3,4) P_2 and PtdIns (4,5) P_2 was also detected, but binding to monophosphorylated PtdIns was not (data not shown). The relative affinities of the SNX1 PX domain for PtdIns phosphates were determined by spotting serial dilutions of the target lipids on membranes. The SNX1 PX domain specifically bound to PtdIns (3,4,5) P_3 with weaker binding to PtdIns (3,5) P_2 (Fig. 5*B*). The PX domain of SNX1 thus binds PtdIns (3,4,5) P_3 with the highest affinity. Preincubation of the PX domain of SNX1 with IP_4 in solution inhibited binding to immobilized PtdIns (3,4,5) P_3 (data not shown), implying that the failure to detect binding to immobilized inositol tetrakisphosphate (IP_4) was due to technical reasons. Specific recognition of PtdIns (3,4,5) P_3 is the same as that of certain PH domains—i.e., Grp1 (25). As confirmed in Fig. 5*F*, the GST-PH domain of Grp1 specifically recognizes PtdIns (3,4,5) P_3.

To assess the importance of conserved residues for recognizing PtdIns, three regions were mutated (Fig. 4*A*) and the purified protein domains were tested in lipid overlay binding assays. As shown in Fig. 5*C*, mutation of the proximal Arg cluster abolished and mutation of the Pro-rich region, and the distal Arg cluster severely impaired binding of the PX domain of SNX1 to PtdIns (3,4,5) P_3. None of the mutations resulted in a change in the pattern of lipid recognition. The specificity of SNX1 PX domain binding in lipid overlay assays was verified using both His-6 and GST fusion proteins in addition to the untagged version (data not shown). Using a liposome-binding assay in which SNX3 recognized PtdIns (3) P, the PX domain of SNX1 showed no specific PtdIns recognition (data not shown). It thus resembles a group of yeast PX domains, including the SNX1 ortholog Vps5p, that demonstrate only low-affinity binding to liposomes (9), indicating that additional components are necessary for high-affinity binding and targeting *in vivo*.

The PX domain of SNX2 (aa 118–266) exhibited lipid-binding specificity that differs from that of SNX1 with a preference for binding to PtdIns (3) P (Fig. 5*D*). SNX3, the structure of which consists principally of a PX domain, also specifically recognizes PtdIns (3) P (Fig. 5*E*), in agreement with Xu *et al.* (6).

Discussion

Targeting of SNX1 to endosomal vesicles is essential for assembly of a complex of proteins that coat such vesicles. Regulated overexpression of the NH_2 terminus of SNX1 containing the PX domain interfered with ligand-induced down-regulation and degradation of EGFR, consistent with inhibition of the function of endogenous SNX1. Overexpression of holo SNX1, which was initially isolated via interaction with a lysosomal targeting code in EGFR, enhanced degradation of EGFR (10). Because the NH_2 terminus of SNX1 did not affect the rate of ligand-induced

endocytosis of EGFR, it is likely that SNX1 and associated proteins direct vesicular trafficking and protein sorting in the endocytic compartment (24). SNX proteins are reported to interact with a variety of cell surface receptors (10, 11, 26), suggesting that interactions with vesicle cargo, in addition to membrane lipids and other proteins, are important in their function.

Mutational analysis of SNX1 indicates that both an intact PX domain that recognizes PtdIns and an intact helical COOH terminus involved in protein·protein interactions are necessary for proper subcellular localization of holo SNX1. Deletion or point mutations in the PX domain of SNX1 that correspond to residues that are essential for binding of PX domains to PtdIns (3) P (2–8) abrogated localization of SNX1 to vesicles. The mutations studied correspond to conserved residues that play essential roles in lipid recognition of the $p40^{Phox}$ PX domain (27). NMR studies of the Pro loop of Vam7p (2) are consistent with this loop being an essential part of the specificity of lipid binding by PX domains (27). This region may also mediate interaction with SH3 domains (28).

The requirement of PI 3-kinase activity for vesicle localization of SNX1 indicates that the D3 phosphate is essential for PtdIns recognition. Because PtdIns (3) P is a well established lipid modification in endosomes (8), the observation that the SNX1 PX domain specifically recognized PtdIns (3,4,5) P_3 was unexpected because it is principally localized to the plasma membrane where it assembles PH domain-containing proteins (29). Yu and Lemmon proposed that "low-affinity" PX domains provide specificity in localization but that other targets are needed besides PtdIns (3) P to drive membrane association (9). Mutation of the coiled-coil COOH terminus of SNX1 abolished vesicle localization, indicating that the COOH terminus is also necessary for vesicle localization. We propose that both the PX and coiled-coil domains of SNX1 are necessary for proper vesicular localization. Teasdale *et al.* (12) also concluded that the COOH terminus of SNX1 was necessary for vesicle localization.

SNX1 forms a complex with a number of proteins (16) in addition to SNX2, and these proteins likely play an important role in SNX1 localization and function. It is possible that in heterodimeric complexes SNX2 recognition of PtdIns (3) P plays an important role in endosomal vesicle localization. Binding to Hrs, whose FYVE domain localizes it to early endosome (30), may also play a role. We cannot exclude the presence of a small pool of PtdIns (3,4,5) P_3 in endosomes, because both PI 4-kinase and PI4 (P) 5-kinase are constitutively associated with EGFR (31) and provide a mechanism for generating PtdIns (3,4,5) P_3 in membranes that contain EGFR.

The present data support the proposed function of SNX1 in sorting cargo in the endosome pathway to lysosomes. Overexpression of other SNX family members—e.g., SNX3—blocks trafficking in the endosome compartment, including trafficking of EGFR, with concomitant enlargement of vesicles and mixing of compartment contents (6). This finding suggests that SNX3 may function as an endogenous inhibitor of other PX-domain proteins. Data with overexpression of holo SNX1 (10) and with the NH_2 terminus of SNX1 as an inhibitor indicate more specific effects on vesicular trafficking. Understanding the molecular complexes associated with each SNX protein should provide further insights.

We thank Richard Kurten for the SNX2 clone, Carol Renfrew Haft for the SNX3 clone, James Feramisco and Brian Smith for deconvolution microscopy, Michael McCaffrey for electron microscopy, Lora Burns for analytical ultracentrifugation, and Marilyn Farquhar for helpful discussions. This study was supported by National Institutes of Health Grant PO1CA 58689 and California Breast Cancer Research Program Grant 2RB-0216. S.D.E. is an investigator of the Howard Hughes Medical Institute.

1. Pointing, C. P. (1996) *Protein Sci.* **5,** 2353–2357.
2. Cheever, M. L., Sato, T. K., deBeer, T., Kutateladze, T., Emr, S. D. & Overduin, M. (2001) *Nat. Cell Biol.* **7,** 613–618.
3. Kanai, F., Liu, H., Field, S. J., Akbary, H., Matsuo, T., Brown, G. E., Cantley, L. C. & Yaffe, M. B. (2001) *Nat. Cell Biol.* **3,** 675–679.
4. Ellson, C. D., Gobert-Gosse, S., Anderson, K. E., Davidson, K., Erdjument-Bromage, H., Tempst, P., Thuring, J. W., Cooper, M. A., Lim, Z. Y., Holmes, A. B., *et al.* (2001) *Nat. Cell Biol.* **3,** 679–684.
5. Song, X., Xu, W., Zhang, A., Huang, G., Liang, X., Virbasius, J. U., Czech, M. P. & Zhou, G. W. (2001) *Biochemistry* **40,** 8940–8944.
6. Xu, Y., Hortsman, H., See, L., Wong, S. H. & Hong, W. (2001) *Nat. Cell Biol.* **3,** 658–666.
7. Xu, J., Liu, D., Gill, G. N. & Songyang, Z. (2001) *J. Cell Biol.* **154,** 1–7.
8. Sato, T. K., Overduin, M. & Emr, S. D. (2001) *Science* **294,** 1881–1885.
9. Yu, J. W. & Lemmon, M. A. (2001) *J. Biol. Chem.* **276,** 44179–44184.
10. Kurten, R. C., Cadena, D. L. & Gill, G. N. (1996) *Science* **272,** 1008–1010.
11. Haft, C. R., de la Luz Sierra, M. L., Barr, V. A., Haft, D. H. & Taylor, S. I. (1998) *Mol. Cell. Biol.* **18,** 7278–7287.
12. Teasdale, R. D., Loci, D., Houghton, F., Karlsson, L. & Gleeson, P. A. (2001) *Biochem. J.* **358,** 7–16.
13. Zheng, B., Ma, Y.-C., Ostrom, R. S., Lavoie, C., Gill, G. N., Insel, P. A., Huang, X.-Y. & Farquhar, M. G. (2001) *Science* **294,** 1939–1942.
14. Howard, L., Nelson, K. K., Maciewicz, R. A. & Blobel, C. P. (1999) *J. Biol. Chem.* **274,** 31693–31699.
15. Seaman, M. N., McCaffery, J. M. & Emr, S. D. (1998) *J. Cell Biol.* **142,** 665–681.
16. Haft, C. R., de la Luz Sierra, M. L., Bafford, R., Lesniak, M. A., Barr, V. A. & Taylor, S. I. (2000) *Mol. Biol. Cell* **11,** 4105–4116.
17. Dowler, S., Currie, R. A., Campbell, D. G., Deak, M., Kula, G., Downes, C. P. & Alessi, D. R. (2000) *Biochem. J.* **351,** 19–31.
18. McCaffery, J. M. & Farquhar, M. (1995) *Methods Enzymol.* **257,** 259–279.
19. Gossen, M. & Bujard, H. (1992) *Proc. Natl. Acad. Sci. USA* **89,** 5547–5551.
20. Burke, P., Schooler, K. & Wiley, H. S. (2001) *Mol. Biol. Cell* **12,** 1897–1910.
21. Wiley, H. S., Herbst, J. J., Walsh, B. J., Lauffenburger, D. A., Rosenfeld, M. G. & Gill, G. N. (1991) *J. Biol. Chem.* **266,** 11083–11094.
22. Wiley, H. S. & Cunningham, D. D. (1982) *J. Biol. Chem.* **257,** 4222–4299.
23. Barr, V. A., Phillips, S. A., Taylor, S. I. & Haft, C. R. (2000) *Traffic* **1,** 904–916.
24. Kurten, R. C., Eddington, A. D., Chowdhury, P., Smith, R. D., Davidson, A. D. & Shank, B. B. (2001) *J. Cell Sci.* **114,** 1743–1756.
25. Klarlund, J. K., Guilherme, A., Holik, J. J., Virbasius, J. V., Chawla, A. & Czech, M. P. (1997) *Science* **275,** 1927–1930.
26. Parks, W. T., Frank, D. B., Huff, C., Haft, C. R., Martin, J., Meng, X., de Casestecker, M. P., McNally, J. G., Reddi, A., Taylor, S. I., *et al.* (2001) *J. Biol. Chem.* **276,** 19332–19339.
27. Bravo, J., Karathanssis, D., Pacold, C. M., Pacold, M. E., Ellson, C. D., Anderson, K. E., Butler, P. J, G., Lavenir, I., Perisic, O., Hawkins, P. T., *et al.* (2001) *Mol. Cell* **8,** 829–839.
28. Hiroaki, H., Ago, T., Ito, T., Sumimoto, H. & Kohda, D. (2001) *Nat. Struct. Biol.* **8,** 526–530.
29. Stokoe, D., Stephen, L. R., Copeland, T., Gaffney, P. R. J., Reese, C. B., Painter, G. F., Holmes, A. B., McCormick, F. & Hawkins, P. T. (1997) *Science* **277,** 567–570.
30. Komada, M. & Soriano, P. (1999) *Genes Dev.* **13,** 1475–1485.
31. Cochet, C., Folhol, O., Payrastre, B., Hunter, T. & Gill, G. N. (1991) *J. Biol. Chem.* **266,** 637–644.